

Sublimation Rate of TNT Micro-Crystals in Air

Journal:	<i>The Journal of Physical Chemistry</i>
Manuscript ID:	jp-2010-05168h.R2
Manuscript Type:	Article
Date Submitted by the Author:	n/a
Complete List of Authors:	Zeiri, Yehuda; Ben-Gurion University Gershanik, Arcady; Ben-Gurion University

SCHOLARONE™
Manuscripts

Sublimation rate of TNT micro-crystals in air

Arcady P. Gershanik^a and Yehuda Zeiri^{a,b}.*

^a Biomedical Engineering, Ben Gurion University of the Negev, Beer-Sheva 84105, Israel

^b Division of Chemistry, NRCN Beer-Sheva P.O. Box 9001, 84190, Israel

arcady@bgu.ac.il, yehuda@bgu.ac.il

Corresponding author is Yehuda Zeiri

ABSTRACT

Reliable measurements of non-uniform layers of Trinitrotoluene (TNT) micro-crystals sublimation rate were carried out using a quartz crystal microbalance (QCM). The sample layer was prepared by precipitation of TNT from a well defined volume of its solution in acetonitrile. The TNT solution was placed on the QCM electrode surface to form the precipitated layer of TNT micro-crystals. It is shown that the kinetics of small TNT particles sublimation is controlled by the molecular diffusion in air. The sublimation process is well described by simple diffusion expressions which are discussed in the literature for both individual hemispherical shaped micro-crystals and disk-shaped layers. Expressions describing particle size evolution in time were derived based on this diffusion model. It is shown that the expressions developed can be used to simulate particle sublimation in a wide size range, including very small sub-micron particles.

1. Introduction

1
2
3 For over a decade large amounts of governmental resources are channeled into the war against
4 terrorism by most of the countries all over the globe. Large efforts are devoted to maintain a secure
5 public transportation in particular the air traffic. The meaning is to do all that one can to eliminate the
6 possibility of smuggling explosives into airports and airplanes. The problem is that the vapor pressure of
7 most solid explosives, both military and improvised, is too low to detect their presence using methods
8 that examine their gas phase existence. Thus, the most promising way to detect the explosive is to
9 sample micron (or less) size explosive particles that may be found on the belongings or cloth of people
10 that were exposed to explosive in manufacturing or assembling laboratories. The sampling in most cases
11 is performed by a swipe of the examined surface using a swipe material and detecting the existence of
12 explosives on the swipe material by an Ion Mobility spectrometer (IMS).
13
14
15
16
17
18
19
20
21
22
23
24

25
26 The fate of explosive particles on various substrates related to terrorist or criminal acts is important if
27 one desires to optimize the sampling of explosive particles. As in an open system, explosive and all kind
28 of particles, are expected to evaporate and disappear, hence, knowledge of their lifetime in various
29 environmental conditions is important. For most solid explosive the vapor pressure is rather low and its
30 evaporation in air may occur during a relatively long time scale. Particle's lifetime is of interest since it
31 determines the possibility to sample and detect particles in various scenarios related to terrorist and
32 criminal activities. Moreover, knowledge of the sublimation rate dependence on the particle dimension
33 would give the possibility of restoring of their initial distribution at given environmental conditions.
34
35
36
37
38
39
40
41
42
43
44

45 The sublimation process is based on two fundamental events, the first is desorption of molecules from
46 the solid and the second is the motion of the gas phase molecules into the surrounding and away from
47 their original source. This description is valid only if the desorption process is a reversible one, namely,
48 the desorbing molecules do not alter chemically in a non reversible manner (i.e., they do not
49 decompose).
50
51
52
53
54
55
56
57
58
59
60

1 If the sublimation source constitute of small particles, additional considerations have to be taken into
2 account. Among these are the role of air flow on the diffusion process and the enlarged deviation from
3 equilibrium of the maximal vapor concentration in vicinity of solid.
4

5
6
7 As will be discussed below, the estimate of sublimation rate based on diffusion equations requires
8 knowledge of the diffusion coefficients of the sample molecules in air and the values of the sample
9 saturation vapor pressures. As mentioned, the vapor pressure values of most explosives are quite low.
10
11 As a result, considerable discrepancies of up to factor 2-3 and sometimes more are found in the
12 published experimental data¹⁻⁶. The experimental reports of the TNT diffusion coefficient in air also
13 differ. The variation between the reported values for TNT diffusion in air⁷⁻⁹ spans up to 30%. The
14 theoretical estimations of the diffusion coefficient by several different methods differ by a factor of 3.¹⁰
15
16

17
18
19 Contrary to the nature of the sublimation process discussed above, a recent publication, related to TNT
20 sublimation, suggested that influence of the diffusion-in-air retardation on the overall rate is
21 negligible¹¹. It will be demonstrated that the description of TNT sublimation kinetics as a diffusion
22 process agrees well also with the experimental results of Ref. ¹¹
23

24
25
26 The quartz crystal microbalance (QCM) is a suitable instrument to measure sublimation rates due to
27 its very high sensitivity to minute mass changes, of the order of sub-nanograms. However, QCM can be
28 used only if some requirements related to the physical, chemical and mechanical properties of the
29 sample are met. In general, the substance under investigation should have good adhesion to the QCM
30 surface, should be homogeneously spread and be sufficiently rigid.^{12,13} QCM may lose its high
31 sensitivity in the absence of good adhesion or undergo additional frequency shifts in the case of soft
32 sample due to dissipation of oscillation energy.^{14,15} Large errors in the measurement may occur in the
33 case of thick non-rigid layers due to the acoustic wave absorption by the soft load.
34
35

36
37
38 In this work we used a quartz crystal microbalance (QCM) to study the sublimation rate of
39 trinitrotoluene (TNT) micro-crystals. The micro-crystals layer was directly precipitated from solution
40 onto the QCM electrode surface. The main goal in this study is to understand the mechanism governing
41 the TNT sublimation process and develop an appropriate model to quantify it.
42
43
44
45
46
47
48
49
50
51
52
53
54
55
56
57
58
59
60

2. QCM measurements

2.1 General consideration

It is known from the literature¹³ that the frequency shift of the QCM that is caused by a non-uniform load is equal to the sum of the partial shifts resulting from the mass distributed over the QCM surface. A different sensitivity at different points of the QCM electrode should be taken to account, i.e.

$$\Delta f = \int_0^{2\pi} \int_0^{r_q} \xi(r, \theta) \rho_s(r, \theta) dr d\theta \quad , \quad (1)$$

where Δf is the measured frequency shift relative to the fundamental, r and θ the polar coordinates of different points along the crystal surface, r_q is the electrode radius, ρ_s the density of the sample mass, ξ is a local sensitivity function that is independent on the magnitude of the mass in the approximation of small loads.

Extracting the average value of the sensitivity $\bar{\xi}$ and of the mean sample density along the QCM surface $\bar{\rho}_s$ from the integral (1) one obtains

$$\Delta f = \bar{\xi} \bar{\rho}_s \int_0^{2\pi} \int_0^{r_q} F(r, \theta) dr d\theta = -\frac{\bar{\xi} m}{A} B, \quad (2)$$

with

$$B = \int_0^{2\pi} \int_0^{r_q} F(r, \theta) dr d\theta \quad (3)$$

where A is the QCM electrode surface area and $F(r, \theta)$ represents the reduced distribution function of the load which is independent of the absolute value of mass.

When the distribution is homogenous (i.e., $B=1$), equation (2) is essentially identical to Sauerbrey's equation.¹² In the inhomogeneous mass distribution case, the B value may change from one sample to another but can be assumed to be almost constant during the initial stages of the sample sublimation, before the reduced mass distribution function changed appreciably. In such situation, equation (2) can be rewritten in the following form to describe the sublimation process

$$\Delta(\Delta f) = -\frac{\overline{\xi \Delta m}}{A} B \quad (4)$$

$$\frac{\Delta(\Delta f)}{\Delta f_0} = -\frac{\Delta m}{m_0} \quad (5)$$

where Δf_0 is initial frequency shift after deposition of the initial mass m_0 on the electrode surface.

Thus, measurement of the resonance frequency shift following sample loading allows one to detect the changes in the sample due to evaporation. This type of measurement can yield satisfactory means to study the sublimation rate of various materials of interest.

The accuracy of this approach to measure life time of particles has been examined here using several means. First, the reproducibility of the measurements was examined following consecutive loading of the QCM surface by samples. The good reproducibility obtained in the sublimation rate measurements confirms our assumption concerning the strength of the sample adhesion to the QCM electrode surface. However, the data analysis can be complicated by a strong dependence of the measured evaporation rates on the detailed structure of the sample micro-crystals layer. Hence, a verification of the sublimation rate measurement approach was obtained by comparison between the data obtained by QCM with an independent measurement of the evaporation rate using an analytic balance (ViBRA).

2.2 Experimental procedure

TNT solution

Military standard 2,4,6-trinitrotoluene solution in acetonitrile with TNT concentration of 10 g/l and acetonitrile purity of 99.9% was received from Rafael Ltd. This TNT concentration was found to be too high to obtain reproducible micro-crystal layers. Good reproducibility of the sample layer has been achieved with a more diluted TNT solution (2 g/l). The initial sample layer was created by TNT micro-crystals precipitation during the evaporation of the solvent from 10 μ l TNT solution placed on the QCM electrode. The solvent was allowed to evaporate at room temperature. The micro-crystalline layer formed during solvent evaporation was documented by an optical microscope at various magnifications.

Equipment and procedure

1
2
3 The quartz microbalance used is model QCM100 by Stanford Research Systems, Inc. The AT-cut disk-
4
5 shaped quartz crystal of 1 inch diameter was covered in the central area (0.5 inch diameter) by a thin
6
7 gold layer. According to the manufacturer data, the crystal holder withstands temperature up to 85°C.
8
9 However, the preamplifier attached by a BNC connection to the crystal holder may be exposed only to
10
11 temperatures up to 40°C. To eliminate this restriction, in all experiments reported here the preamplifier
12
13 was separated from the crystal holder by a 10 inch long cable. The temperature control was achieved by
14
15 placing the crystal holder with the sample on the crystal surface in an oven with polished stainless steel
16
17 walls with ventilation located at the top of the oven. Before placing the sample in the oven it was heated
18
19 to the desired temperature. The sublimation experiments reported below were carried out at constant
20
21 temperature with fluctuations less than $\pm 0.2^\circ\text{C}$.
22
23
24
25

26 The quartz crystal holder was usually placed on the bottom of the oven at a distance 5-6 cm from one of
27
28 the walls with the sample facing the wall. The position of the crystal was chosen to be as far as possible
29
30 from the ventilator. After placing the crystal holder in the oven at the desired temperature, the crystal
31
32 and the sample reached the desired temperature within approximately 5 minutes. The beginning of the
33
34 data acquisition was delayed by this period.
35
36
37

38 To eliminate the accumulation of the TNT vapors in the volume above the sample during the
39
40 sublimation process, the oven was pumped out continuously using a small membrane pump (pumping
41
42 rate of 18 L/min).
43

44 As mentioned above, to verify the results obtained using the QCM experiments, we performed a similar
45
46 experiment using an analytical balance. This experiment was carried out in the following way. A layer of
47
48 TNT was precipitated on both sides of a large thin plastic disc (diameter of 100 mm) using the 2 g/l
49
50 TNT solution in acetonitrile. The total amount of TNT precipitated on the sample plate was 15 mg. The
51
52 sample was placed in the oven on the disc ledge, with both faces available for evaporation, at
53
54 temperature of $T=30^\circ\text{C}$. The change in the disc weight was measured every hour to obtain a direct
55
56 measure of the fraction evaporated from the TNT layer.
57
58
59
60

2.3 Results

1
2
3 A typical optical microscope image of the initial TNT layer near the central part of the QCM electrode is
4
5 shown in Fig. 1. One can see clearly that the initial morphology of the TNT layer is composed of well
6
7 separated TNT micro-crystals. Simple image analysis of many images such as the one shown in figure 1,
8
9 at different magnifications, allowed us to obtain an estimate of the average micro-crystal diameter and
10
11 the average distance between neighboring micro-crystals. In the image analysis the particle area is
12
13 measured and converted to diameter approximating the shape by a circle. The average diameter of these
14
15 micro-crystals was found to be in the range of 10-12 micrometers. The average distance between
16
17 neighboring particles was found to be of the order of 100 μm , much larger than the particles diameters.
18
19 The corresponding standard deviations of these two quantities are: 20% and 36% respectively.
20
21

22
23 To obtain information about to the height of the TNT micro-crystals, stylus surface profiler (Dektak 8)
24
25 was used. This system offers flexible stylus forces normal to the substrate of 0.03 mg with height
26
27 resolution of 0.75nm. The profiler software allows simultaneous observation through the microscope of
28
29 the particle together with the stylus. This feature helps to ensure that the stylus do not move the particle.
30
31 The typical height variation along an arbitrary line across the sample is shown in Fig. 2. The average
32
33 height of the TNT micro-crystals obtained is 5.9 μm with a standard deviation of 0.9 μm .
34
35

36
37 Ideally, one would like have a layer composed of identical particles that would enable an easier
38
39 understanding of the system behavior. Unfortunately, this is impossible for layers that are formed by
40
41 precipitation process. Moreover, a full statistical treatment using the particle geometry distribution
42
43 cannot be carried out due to the unknown dependence of the QCM sensitivity on the location of the
44
45 various particles. Analysis of the optical microscope images together with the profiler data clearly shows
46
47 that the precipitated layer consists, to a very good approximation, of separated particles whose average
48
49 radius and height is approximately 6 μm . It is clear that the actual shape of the particles exhibits wide
50
51 variations due to the nature of the process used to form the layer. However, in the following a simple
52
53
54
55
56
57
58
59
60

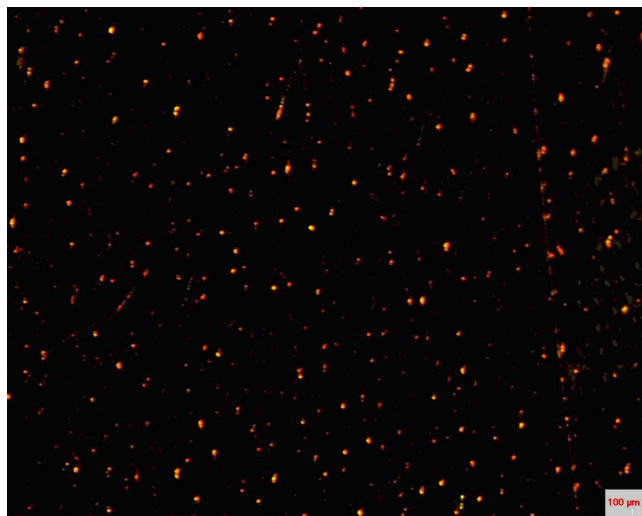


Figure 1. Typical optical microscope image of the TNT micro-crystal layer near the central part of QCM electrode following precipitation of the micro-crystals from a 2 g/l solution

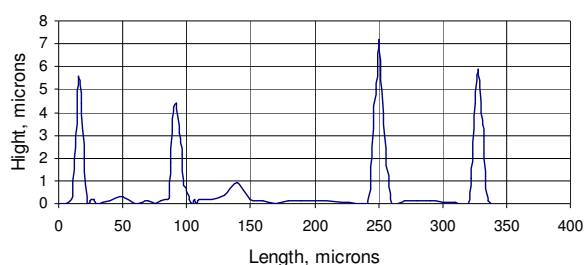


Figure 2. Typical spectrum of the TNT micro crystal layer near the central part of QCM electrode as obtained by the Dektak profiler measurements

model to describe the sublimation rate of the micro-particles will be described. To keep this model simple we shall approximate the shape of the individual particles by hemispheres with radius of 6 μm . It will be demonstrated that this approximation allows to obtain reasonable agreement between the experimental data and the model predictions. Some of the uncertainties associated with the various approximations used will be further discussed below.

The mass fraction change during the sublimation process as measured by the QCM is shown in Figure 3 for four different temperatures. Two points should be noted: (i) Measurements in which the analytical balance was used to monitor weight change at 30°C confirm the reliability of the data obtained by the QCM. This substantiates the validity of evaporation rate measurements using the QCM. (ii) The air flow

1 induced by the oven ventilator does not lead to significant changes in the measured evaporation rate. .

2
3 The reproducibility of the QCM measurements at any given temperature is very good achieving $\pm 7\%$ of
4
5 the measured value at highest temperature 50°C and $\pm 15\%$ at the lowest temperature 30°C . These results
6
7 suggest that the approach used for sample preparation yield statistically similar initial sample layer
8
9 morphologies. The Blue and Magenta curves in Fig. 3 corresponds to two experiments carried out at
10
11 40°C , first with sample placed facing the oven wall and far from the ventilator (Magenta) and the other
12
13 with sample placed as close as possible to the ventilator in the oven (Blue). The results of these two
14
15 experiments show deviations of approximately 20%. This deviation is somewhat greater than in the
16
17 other measurements performed at 30°C and 50°C . However, this deviation is mainly related to the
18
19 thermo-mechanical action of the air flow on the QCM.
20
21
22

23
24 The initial slope of the various curves in Fig. 3 is related to the evaporation rate of the sample. The
25
26 magnitude of the initial slopes, marked on Fig. 3, was obtained by a linear fit of the sublimated mass
27
28 curves in their linear regions.
29

30
31 If one assumes an Arrhenius form for the temperature dependence of evaporation rates, then the
32
33 activation energy of the process can be obtained from the slope of the linear dependence between natural
34
35 logarithm of the sublimation rate and of inverse absolute temperature. Figure 4 shows the experimental
36
37 points together with the best fit of linear variation line. The activation energy, related to the slope,
38
39 associated with the TNT sublimation process is 97 ± 7 kJ/mol. This value is very close to the heat of
40
41 sublimation 99 kJ/mol obtained in¹ but considerably smaller than the largest among the reported values¹⁻
42
43
44
45 ⁶ of 141 kJ/mol.⁶
46
47
48
49
50
51
52
53
54
55
56
57
58
59
60

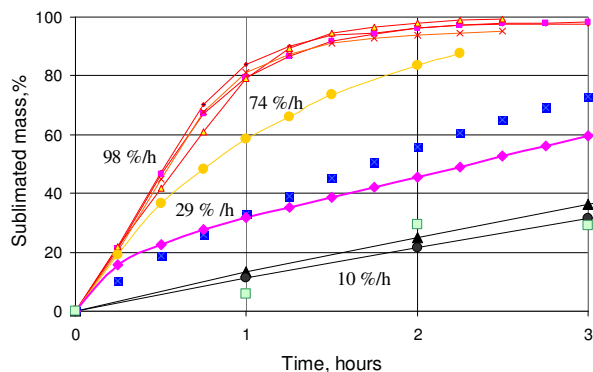


Figure 3. Sublimation rate of the precipitated TNT layer measured by QCM at several temperatures: red lines – corresponds to 50°C, yellow - corresponds to 45°C, magenta - corresponds to 40°C, and black - corresponds to 30°C. Blue rectangles correspond to data obtained in an experiment at 40°C with the sample positioned as close as possible to the ventilator in the oven. The green points correspond to data obtained in the experiment using the analytical balance to follow weight changes. Numbers adjacent to the curves indicate the average value of the initial sublimation rate.

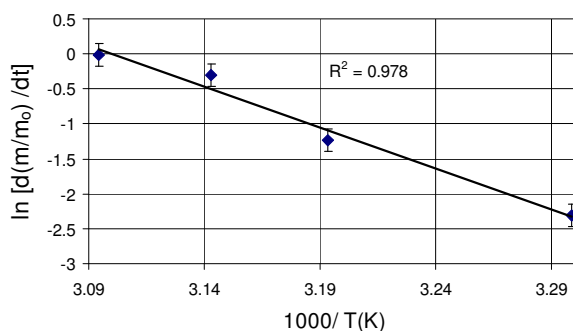


Figure 4. Dependence of the initial sublimation rate on inverse temperature

3. Discussion

The sublimation process consists at least of two sequential basic events: a stage of the molecules escaping (desorption) from the solid and the motion of these molecules away from the vicinity of the solid. These two stages are considered in more details below.

3.1 The desorption process

The rate of molecules escaping from solid is easily calculated from the value of equilibrium vapor pressure using the well known Langmuir-Knudsen approach for vapor pressure measurements^{16,17} that gives

$$-\frac{dm}{dt} = g \frac{A_0 P_{sat}}{\sqrt{2\pi M k_B T}}, \quad (6)$$

where dm/dt is the rate of sample mass change due to the sublimation, A_0 denotes the sample surface area, P_{sat} is the saturation vapor pressure of the sample material, T - is the temperature, k_B is Boltzman's constant, M is the molecular mass, and g represent the sticking coefficient that usually considered as close to unity.

To the best of our knowledge, the experimental values of sticking coefficient for TNT were not reported in literature. Moreover, all the vapor pressure measurements¹⁻³ which were carried out by the Knudsen approach assumed that $g=1$. In other words, the reported vapor pressure data are really a measure of the product gP_{sat} rather than of P_{sat} by itself. Therefore, using the vapor pressure data obtained in the Langmuir-Knudsen type experiments allows replacing of the product gP_{sat} by the experimentally obtained effective P_{sat} .

For a hemispherical particle of radius r_0 and initial mass m_0 one can rewrite equation (6) in the following form

$$-d(m/m_0) = \frac{3P_{sat}}{r_0 \rho} \sqrt{\frac{M}{2\pi k_B T}}, \quad (7)$$

where ρ represents the sample density.

Equation (7) relates to a hemispherical particle, i.e., the shape that possess the smallest ratio of surface area to volume (or mass). Consequently, the calculations can be regarded as a lower limit for the evaporation rate since any deviation from the hemi-spherical particle shape corresponds to larger surface volume ratio. To estimate the minimal TNT mass loss rate according to equation (7) at 30°C we used the

largest and the smallest vapor pressures reported in the literature¹⁻⁶. The largest reported value of TNT vapor pressure is 2.38×10^{-3} Pa¹ which yields an evaporation rate of 0.27 %/s while the smallest value, $P_{\text{sat}} = 1.05 \times 10^{-3}$ Pa, reported by Oxley et al.⁴ yields a sublimation rate of 0.12 %/s. The corresponding measured rate in the QCM experiments was 2.8×10^{-3} %/s. This discrepancy of about two orders of magnitude suggests that most of the desorbing TNT molecules are re-adsorbed by the solid after collisions with the surrounding air molecules. As a result, in the near vicinity of the particle surface an equilibrium concentration of the sample molecules is maintained. Thus, to describe properly the evaporation process one needs to take into account the diffusion of the sample molecules in the surrounding air using the boundary condition described above. This second stage of the sublimation process is discussed below.

3.2 Diffusion in air

Let us consider the diffusive motion of sample molecules in the gas phase after their desorption from the TNT micro-crystal surface. It is assumed that molecular diffusion is the main process that governs the motion of the sample molecules while they leave the particle vicinity. In other words, various air flows leading to convective or forced motion are neglected. This is justified due to the nature of the flow near small particles as discovered and measured experimentally by Langmuir¹⁸. Below we will present a quantitative estimation of the particle dimension which satisfies these conditions.

Let us consider the quasi-stationary steady state diffusion process. The solution of the Fick's first law of molecular diffusion for a hemispherical particle that is placed on a substrate has the form¹⁹

$$C(r) = C_{\text{max}} \frac{r_0}{r} \quad (8)$$

where C_{max} represents the concentration of the sample molecules in the gas phase next to the particle surface, r_0 is the particle radius, and r is the independent variable in the range r_0 to infinity.

According to (8) the gas phase molecular concentration $C(r)$ decreases along the radial direction as $1/r$. At small distances from the particle, of order of ten times the particle radii, the concentration $C(r)$

1 becomes negligibly small relative to C_{\max} . In other words, the main resistance to the diffusion process is
2 most effective in the region next to the particle surface. If this region is within the limits of the boundary
3 layer (a motionless gas layer whose width can vary in the range of few micrometers up to few
4 millimeters or more depending on the conditions in the system) then, to a very good approximation, air
5 flow is not expected to alter the concentration of TNT molecules and their transport. The small volume
6 of this region requires only very small amount of sublimated substance to achieve steady-state gas
7 molecules concentration. This is especially true in case of TNT and similar substances with low vapor
8 pressure. For example the density of the solid TNT is approximately 10^{10} times greater than the density
9 of its saturate vapor at room temperature.
10
11
12
13
14
15
16
17
18
19

20 Remembering that for ideal gas
21
22

$$23 \quad C_{\max} = \frac{P_{sat}}{k_B T} \quad (9)$$

24
25
26
27
28
29 Substitution of eqs. (8) and (9) into Fick's first law expression, one obtains for the sublimation rate the
30 following expression for hemispherical particle
31
32

$$33 \quad -\frac{dm}{dt} = \frac{2\pi D P_{sat} r_0}{k_B T} \quad (10)$$

34
35
36
37
38 where D denotes the TNT diffusion coefficient in air. For the fractional mass change one obtains
39

$$40 \quad -d(m/m_0)/dt = \frac{3DP_{sat}M}{r_0^2 \rho k_B T} \quad (11)$$

41
42
43
44
45 Equation (11) describes the fractional mass change for hemispherical particle was applied to model
46 the sublimation rate of TNT particles investigated here. The coefficient 3 in eq. (11) can be regarded as
47 a form-factor related to the hemispherical form of the particles. This form factor is an approximation of
48 the actual mean statistical form-factor of the precipitated TNT layer whose exact value is unknown. To
49 the best of our knowledge, analytical forms of the steady state solutions of Fick's equation for the vapor
50 diffusion from a small source are available in literature only for hemispherical and disk shaped
51 sources²⁰. Therefore the form factor for an arbitrary shaped particle is not available. According to Grey
52
53
54
55
56
57
58
59
60

1 et al.²⁰ the corresponding sublimation rate equation for a disk of radius r_d is given by the following
2 expression
3

$$4 \quad -dm/dt = \frac{4DP_{sat}r_d}{k_B T} \quad (12)$$

5
6
7
8

9 Comparison with equation (10) for the mass loss by a hemispherical particle source shows that the form
10 factor for hemisphere is $\pi/2$ times greater than that for a disk shaped source. This difference can serve as
11 an approximate measure of the form-factor variation for different shape particles.
12
13

14 Knowledge of the saturated vapor pressures and the magnitude of the diffusion coefficients for TNT are
15 required. However, saturated vapor pressures reported in the literature show (see discussion above) large
16 discrepancies, up to factor of 2-3¹⁻⁶. For TNT diffusion coefficient the reported values show discrepancy
17 of about 30%.⁷⁻⁹ Therefore for the analysis described below we use an average value of the diffusion
18 coefficients reported in the literature⁷⁻⁹, $D=5.59 \cdot 10^{-6}$ m²/s, and neglect its slight temperature dependence
19 in the narrow temperature range studied here.
20
21

22 The vapor pressure data reported in the literature¹⁻⁶ are shown in Figure 5 for the temperature range of
23 25°C-50°C. It is quite clear that this data can be subdivided into two main groups (Refs. ¹⁻³ and Refs. ⁴⁻⁶)
24 with considerably different slopes. Note that all vapor pressure values seem to converge to the same
25 value near 50°C. The difference in the slopes of these two groups reflects the corresponding difference
26 in the heat of sublimation values, 99 kJ/mol and 141 kJ/mol respectively. The source of this difference is
27 unclear to us. Our estimate of the heat of sublimation to be 97 kJ/mol (see Figure 4) is close to the data
28 of the first group (the low slope group).¹⁻³
29

30 The calculated sublimation rates, using all the reported vapor pressure, are summarized in Tables 1a and
31 1b together with the measured rates as obtained in the QCM experiments. The calculated rates, using all
32 the P_{sat} values of Refs ¹⁻⁶ yield a sublimation rate whose magnitude is approximately twice the measured
33 rates with only small dependences on temperature. Taking to account the uncertainties of the TNT
34 micro-crystals size and shape distributions the agreement between the measured and calculated values is
35 very satisfactory.
36
37
38
39
40
41
42
43
44
45
46
47
48
49
50
51
52
53
54
55
56
57
58
59
60

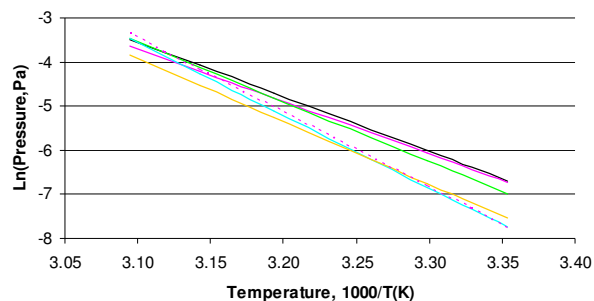


Figure 5. TNT vapor pressure data in the temperature range 25°C-50°C: black line presents data of Linchitz et al.¹, red line-of Pella², green line-of Cundall et al.³, blue line-of Oxley et al.⁴, yellow line-of Edwards⁵, and magenta line-of Leggett⁶.

Sublimation rates of the TNT samples with a much better definition of the sample initial geometry is presented in the paper of R. Mu et al.¹¹. In their study of the interaction of TNT layers with several substrates, the authors measured the sublimation rate in air of a thin TNT disc shaped layer formed by vapor deposition on the QCM electrode surface. The thickness of the vapor deposited disc in this study was 12 microns with a diameter of 6 mm.

Table 1a

Comparison of calculated and experimental sublimation rates at different temperatures. Table 1a, presents the calculated results using the measured vapor pressures that corresponds to heat of evaporation of 99 KJ/mol (first group in Fig. 5) while Table 1b below presents the calculated values using the vapor pressures that corresponds to heat of evaporation of 141 KJ/mol (second group in Fig. 5).

t, °C	Measured, 1/h	Calculated using vapor pressure of:			Average	Ratio Calc/Meas.
		Lenchitz ¹	Pella ²	Cundall ³		
30	0.1	0.22	0.21	0.18	0.20	2.02
40	0.29	0.78	0.72	0.72	0.74	2.55
45	0.74	1.44	1.29	1.40	1.38	1.86
50	0.98	2.59	2.26	2.67	2.51	2.56

Table 1b

t, °C	Measured, 1/h	Calculated using vapor pressure of:				Average	Ratio Calc/Meas.
		Oxley ⁴	Edwards ⁵	Leggett ⁶	Average		
30	0.10	0.10	0.11	0.10	0.10	1.02	
40	0.29	0.52	0.53	0.68	0.58	1.99	
45	0.74	1.18	1.08	1.60	1.29	1.74	
50	0.98	2.59	2.15	3.66	2.80	2.86	

The description of the sublimation process given here is different than that given by Mu et al.¹¹ despite the fact that the method of measurement is very similar. In the study of Ref.¹¹ the authors neglected the retardation effect of the air on the TNT sublimation from a disc-shaped sample. In the following we shall reanalyze the data obtained by Mu et al.¹¹ using the simple diffusion based description discussed above.

A comparison between the experimental data presented in Ref.¹¹ and the calculated values obtained by equation (12) for a disc shaped sample is shown in Tables 2a and 2b for the first and second groups of reported vapor pressures discussed above. The value of the diffusion coefficient used was taken as an average of the reported data in the literature⁷⁻⁹. The agreement between the calculated values and the measurements is quite good with differences in the range of 9% up to 60% only. It should be noted that the using the vapor pressures that correspond to evaporation heat of 99 KJ/mol yields sublimation rates in very good agreement with the measured values, while using the second group of vapor pressures results in a slightly poorer agreement. These findings suggests that the roughly twofold deviation between the calculated and the measured values is observed in Tables 1a and 1b are mainly due to the inaccuracy introduced by the assumption of identical hemispherical particles. In addition, the rather good agreement between the experimental data and the calculated rates in Tables 2a and 2b suggest that the sublimation rate of TNT for the disc shaped samples¹¹ were also limited by the diffusion process. It should be noted that according to equation (12) the sublimation rate is proportional linearly to the

sample dimension. This is in contradiction with the authors DIDP model²¹ where the sublimation rate in air was assumed to be proportional to the sample area.

Table 2a

Comparison of the experimental data of Mu *et al*¹¹ with calculated rates according to equation (12). Table 2a, presents the calculated results using the measured vapor pressures that corresponds to heat of evaporation of 99 KJ/mol (first group in Fig. 5) while Table 2b presents the calculated values using the vapor pressures that corresponds to heat of evaporation of 141 KJ/mol (second group in Fig. 5).

t, °C	Measured, ng/s	Calculated using vapor pressure of:				Average	Ratio Calc/Meas
		Lenchitz ¹	Pella ²	Cundall ³	Average		
25	7.54E-3	7.19E-3	7.34E-3	5.63E-3	6.72E-3	0.89	
30	1.47E-2	1.44E-2	1.40E-2	1.17E-2	1.34E-2	0.91	
40	5.56E-2	5.17E-2	4.74E-2	4.75E-2	4.89E-2	0.88	

Table 2b

t, °C	Measured, ng/s	Calculated using vapor pressure of:			Average	Ratio Calc/Meas
		Oxley ⁴	Edwards ⁵	Leggett ⁶		
25	7.54E-3	2.58E-3	3.24E-3	2.69E-3	2.84E-3	0.38
30	1.47E-2	6.35 E-3	7.00E-3	6.77E-3	6.71E-2	0.46
40	5.56E-2	3.46E-2	3.04E-2	3.92E-2	3.48E-2	0.63

Finally, the conclusion about the leading role of diffusion retardation impact on the sublimation process allows describing the time variation of the TNT particle dimensions due to the sublimation process. Let us turn back to the steady state diffusion expression, equation (10). Assuming the validity of the same steady state quasi-stationary approximation, it is possible to replace the constant radius r_0 of the particle by its time dependent magnitude, $r_0(t)$. This approximation is based on the very large difference between the densities of the solid and the vapor phases. For example, if a volume of 10 particle radii surrounding the particle is filled at 30°C by the saturated vapor pressure of TNT, the amount of TNT molecules

1 required to obtain this concentration leads to a contraction of a hemispherical particle by $5 \cdot 10^{-9}$ of its
2 radius. The evaporation rate of the particle will yield P_{sat} in this volume in approximately $2 \mu\text{s}$.
3
4
5
6

7 Integration of equation (10) over time yields the variation of the particle size as a function of time. After
8 substituting in equation (10) instead of mass, m , the corresponding time dependent value the variation of
9 particle radius can be obtained in the form
10
11
12

$$13 \quad r_0(t) = \sqrt{r_0^2(t=0) - \frac{2DP_{\text{sat}}M}{\rho k_B T} t} \quad (13)$$

14
15
16
17
18
19 Typical variation of TNT particle size at $T=30^\circ\text{C}$ according to equation (13) is shown in Figure 6. It is
20 important to point out that equation (13) cannot be justified for very small particles whose size is
21 comparable with the mean free path of the sample molecules in air, of the order of $0.1 \mu\text{m}$. There are a
22 few reasons that equation (13) is incorrect in such situation, the first, and most important, is that the
23 applicability of expression (8) for the concentration distribution breaks down for very small particles.
24 Expression (8) was derived by rigorous integration of Fick's differential equation in the interval starting
25 at the hemisphere boundary, r_0 , and extends to large arbitrary r values.
26
27
28
29
30
31
32
33
34

35 However, Fick's equation is applicable only at some minimal distance λ from the solid surface, in most
36 cases termed as the mean free path. The molecules escaping from the solid surface, move in this range as
37 free flyers rather than as randomly diffusing walkers. According to the limitations of Fick's theory, the
38 lower limit of integration and the maximal concentration of the sample molecules have to be considered
39 as determined at distance λ from solid. Hence, expression (8) has to be rewritten in the form
40
41
42
43
44
45
46
47

$$48 \quad C(r) = C_{\text{max}} \frac{r_0 + \lambda}{r} \quad (14)$$

49
50
51
52 A second issue that is important for small particles is that the division of equation (10) by the particle
53 surface area, $2\pi r_0^2$, to obtain the diffusion flow from a unit area, diverges as the particle size decreases.
54
55
56
57 This leads to a paradox that the rate of sublimation can exceed the respective rate in vacuum. This
58
59
60

inconsistency can be resolved, if one takes into account the decrease in the maximal concentration of sample molecules near the solid surface as the particle size decreases. It is easy to obtain, using simple

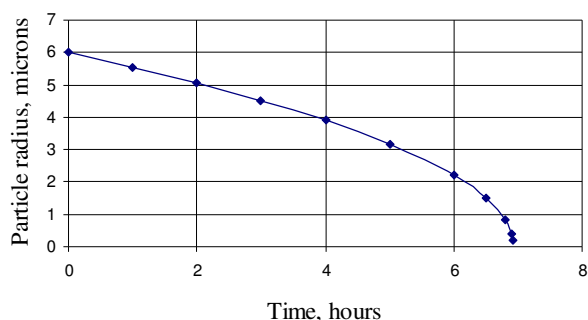


Figure 6. Time dependence of particle radius for a hemispherical TNT particle with initial radius of $6\mu\text{m}$ at 30°C

molecular kinetic theory together with the requirement for material conservation on a hemispherical boundary of radius $(r_0+\lambda)$, the variation of the maximal concentration C_{max} as a function of particle size.

Let us consider the molecular flows at the boundary $(r_0+\lambda)$ of a hemispherical particle as they shown in Figure 7. Three fluxes are considered: F_e , F_r and F_D . These represent the desorption of molecules from solid, the re-adsorption of gas TNT molecules by the solid, and the diffusion of TNT molecules away from the particle respectively. These three fluxes have to be balanced. In the following we assume that sample molecule adsorption onto the substrate surface S can be neglected. It should be noted that including the adsorption of sample molecules onto the substrate would require considering of an additional process of surface diffusion. Since no effects associated with migration of TNT molecules on the substrate surface were observed, this process is neglected. Despite of reflection of the sample molecules from the substrate surface S , the spherical concentration distribution of the gas phase TNT molecules is conserved. Each of the three molecular flows in the Figure 7 can be found from molecular kinetic theory and Fick's equation, i.e.

$$F_e = \frac{A_0 P_{\text{sat}} v}{4k_B T} = \frac{1}{2} \frac{\pi r_0^2 P_{\text{sat}} v}{k_B T}, \quad (15)$$

$$F_r = \frac{A_0 C_{\max} v}{4} = \frac{1}{2} \pi r_0^2 C_{\max} v, \quad (16)$$

$$F_D = -dm/dt = 2\pi D C_{\max} (r_0 + \lambda) \quad (17)$$

where v corresponds to the average thermal velocity that limits the sublimation rate in vacuum and is given by:

$$v = \sqrt{\frac{8k_B T}{\pi M}} \quad (18)$$

Balancing the flows (15)-(17) leads to

$$C_{\max} = \frac{P_{sat}}{k_B T} \left[\frac{1}{1 + \frac{4D(r_0 + \lambda)}{r_0^2 v}} \right], \quad (19)$$

Substitution of equations (19) into (17) leads to the following expression for the sublimation rate, that replaces equation (10)

$$-\frac{dm}{dt} = \frac{2\pi D P_{sat}}{k_B T} \cdot \frac{1}{\left(\frac{1}{r_0 + \lambda} + \frac{4\lambda}{3r_0^2} \right)} \quad (20)$$

with the mean free path λ in air that is related to the diffusion coefficient by.

$$\lambda = \frac{3D}{v} \quad (21)$$

To obtain the particle size variation during sublimation one can integrate equation (20) in a similar manner to the one described above for larger particles, equation (10), to obtain the relation

$$r_0^2 - r(t)^2 + \frac{2}{3} \lambda [r_0 - r(t)] + 2\lambda^2 \ln \left[\frac{r_0 + \lambda}{r(t) + \lambda} \right] = \frac{2DP_{sat}M}{\rho k_B T} t \quad (22)$$

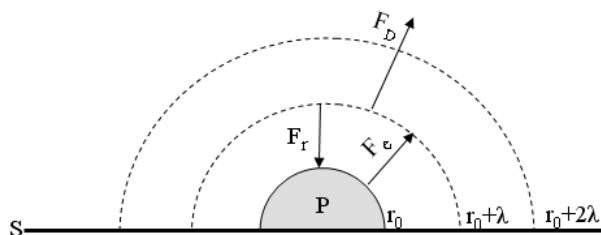


Figure 7. Scheme of molecular flows near the particle boundary and at a surface that is located at a distance λ from the particle P surface. The fluxes: F_e , F_r and F_D are flows associated with molecular desorption from the solid, re-adsorption of molecules to the solid and molecular diffusion away from the solid respectively.

It should be noted that in integrating equation (20), one could take into account the dependence of the saturated vapor pressure on the particle size or on the interaction with a substrate, if required.

One can see that at $\lambda \ll r(t)$ the resultant equation (22) converts into eq. (13).

Figure 8 presents results of numerical calculations according to eq. (22) for a hemispherical TNT particle with an initial radius of $0.2 \mu\text{m}$ at 30°C . The result that would be obtained using eq. (13) is also shown for comparison. The difference in the asymptotic behavior of the two curves is clearly seen. It is obvious that equation (22) leads to a considerably slower sublimation of small (sub micron) particles.

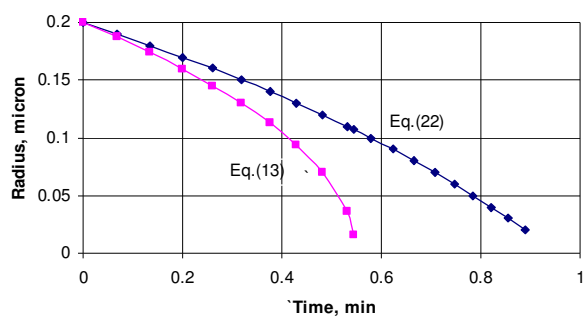


Figure 8. Time dependence of the size variation of a $0.2 \mu\text{m}$ radius hemispherical TNT particle at 30°C

4. Conclusion

We have shown in this study that QCM experiments can be used for the measurement of sublimation rates of non uniform layers of TNT micro-crystals. The TNT particles were approximated as hemispherical micro-crystals based on their measured average diameter and height. The approximation of the TNT particle by a hemispherical shape was crucial for the development of simple analytical expressions. It was demonstrated that sublimation rate of small TNT particles is controlled by molecular diffusion of the TNT vapor in the surrounding air. Comparison with data from the literature related to the sublimation of uniform TNT disc like layers confirms this result. Following this conclusion, we obtained simple expressions to describe the particles size evolution during the sublimation process. The expression obtained to describe the sublimation rate allows the evaluation of the disappearance rate of TNT particles with the appropriate behavior for a wide size range, starting at very small sub-micron particles.

It should be noted that the results of the present study clearly indicates that traces of TNT particles are expected to evaporate after a few days. The actual lifetime of such particles depends on the conditions they are exposed to. This lifetime can be reliably estimated using the expressions developed here.

Acknowledgment

This work was partially supported by The Center of Excellence for Explosives Detection, Mitigation and Response, a Department of Homeland Security Center of Excellence in The University of Rhode Island.

References

1. Lenchitz, C.; Velicky, R.W. *Journal of Chemical and Engineering Data* **1970**, 15, 401-403
2. Pella, P.A. *J. Chem. Thermodynamics* **1977**, 9, 301-305
3. Cundall, R.B.; Palmer, T.F.; Wood C.E.C. *J.Chem.Soc.Farad.Trans.* **1978**, 74, 1339-1345
4. Oxley, Jimmie C; Smith, James L.; Shinde, Kajal; Moran, Jesse *Propellants, Explosives, Pyrotechnics* **2005**, 30, 127-130

- 1 5. Edwards, G. *Trans Faraday Soc.* **1950**, 46, 423-427
- 2
- 3 6. Leggett, D.C. *J. Chrom.* **1977**, 133, 83-90.
- 4
- 5
- 6 7. McKone, T.E.; Daniels J.I. *Regulat. Toxicol. Pharmacol.* **1991**, 13, 36-61.
- 7
- 8
- 9
- 10 8. Phelan, James M; Webb, Stephen W. *Environmental Fate and Transport of Chemical Signatures*
- 11 *from Buried Landmines-Screening Model Formulation and Initial Simulations*; Sandia Report SAND97-
- 12 1426.US-741; Sandia National Laboratories, Albuquerque, Ca., 1997
- 13
- 14
- 15
- 16
- 17 9. Rosenblatt, D.H.; Burrows, E.P.; Mitchell, W.R.; Parmer, D.L.; In Hutzinger O., Ed.; *The*
- 18 *handbook of environmental chemistry*; Springer-Verlag: Berlin, 1989, 195–234
- 19
- 20
- 21
- 22
- 23 10. Dortch, M.; Zakikhani, M. ; Furey, J; Meyer, R.; Fant, S.; Gerald, J. Qasim, M; Fredrickson, H;
- 24 Honea, P.; Bausum, H; Walker, K; Johnson, M. *Data Gap Analysis and Database Expansion of*
- 25 *Parameters for Munitions Constituents*; US Army Corps of Engineers Report ERDC/EL TR-05-16:
- 26 Washington, 2005, 32
- 27
- 28
- 29
- 30
- 31
- 32
- 33 11. Mu, R; Ueda, A; Liu, Y. C; Wu, M; Henderson, D.O; Lareau, R.T; Chamberlain, R.T. *Surface*
- 34 *Science Letters* **2003**, 530, L293–L296
- 35
- 36
- 37
- 38
- 39 12. Sauerbrey, G. *Z. Phys.* **1959**, 155, 206–222.
- 40
- 41
- 42 13. Lu, C.S; Lewis, O. *J Appl. Phys.* **1972**, 43, 4385-4390
- 43
- 44
- 45
- 46 14. Chao, Zhang; Guanping, Feng *IEEE Transactions on ultrasonics, ferroelectrics, and frequency*
- 47 *control* **1996**, 43, 5
- 48
- 49
- 50
- 51
- 52 15. Bandey, Helen L.; Martin, Stephen J.; Cernosek, Richard W.; Hillman, A. Robert
- 53 *Anal. Chem.* **1999**, 71, 2205–2214
- 54
- 55
- 56
- 57
- 58 16. Langmuir, I. *Phys. Rev. Ser. II* **1913**, 2, 329 (W)
- 59
- 60

- 1
2
3
4
5
6
7
8
9
10
11
12
13
14
15
16
17
18
19
20
21
22
23
24
25
26
27
28
29
30
31
32
33
34
35
36
37
38
39
40
41
42
43
44
45
46
47
48
49
50
51
52
53
54
55
56
57
58
59
60
17. Knudsen, M. *The Kinetic Theory of Gases*: Methuen: London, 1950
18. Langmuir, I. *Phys.Rev.* **1918**, 12, 368-370
19. Crank, J. *Mathematics of Diffusion*: Oxford University Press: Oxford, 1975,
20. Gray, A.; Mathews, B. B.; MacRobert, T. M. *A Treatise on Bessel Functions and their Applications to Physics*: Macmillan and Co.Ltd: London, 1931
21. Mu, R.; Ueda, A.; Wu, M.H.; Tung, Y.S; Henderson, D.O.; Chamberlain, R.T; Curby, W;
Mercado, A. *J. Phys. Chem. B* **2000**, 104 (1), 105-109

1 Table of contents

2
3 Sublimation rate of TNT micro-crystals in air

4
5 Arcady P.Gershanik, Yehuda Zeiri

6
7 J. Phys. Chem. A, Articles ASAP (As Soon As Publishable)

8
9 Publication Date (Web): (Article)

